Special Interest Group Meeting on Thermal Issues
Laboratory for Machine Tools and Production Engineering (WZL) of
RWTH Aachen, Germany, February 2020
www.euspen.eu

Real-time estimation of time-dependent heat flux for 3D finite domain employing thermal mode and recursive least square deconvolution

Youyoung Kim[1], Jaeyoon Shim[1], Minsu Kim, Sun-Kyu Lee[1,#]

[1]*School of mechanical engineering, Gwangju Institute of Science and Technology, 123, Cheomdangwagi-ro, Buk-gu, Gwangju, Republic of Korea, 61005*

Corresponding author: Sun-Kyu Lee, skyee@gist.ac.kr

Abstract

This work presents a novel surface heat flux estimation method for the 3D finite domain experiencing dynamic convection and surface heat flux. The thermal mode parameter is adopted to produce a mathematical relation between the surface heat flux history function and the transient temperature response vector with modal superposition method and to locate specific measurement point which can represent transient temperature change of the domain. The direct solution is obtained using the modal superposition method with thermal modes and modal time constants representing thermal characteristics of domain, and the proposed surface heat flux estimation method is derived by the inverse solution applying the novel recursive least square deconvolution (RLSD). As a result, estimation result from experiment presents the root mean square error(RMSE) within 2.5% for the maximum magnitude of measured heat flux history, achieved in only 49 seconds of computing time for long-term estimation of 100 minutes.

Keywords: Estimating, Monitoring

1. Introduction

In the midst of the fourth industrial revolution, an increasingly important technology in the smart factory is sensor-based system monitoring. In particular, the heat input history must be known in order to predict the characteristic behaviour of a machine in the time domain. Once the heat input is identified, the system characteristics can be estimated through a cloud computation in terms of thermal, mechanical, and dynamic performance.

In this work, the thermal modes and eigenvalues from the thermal modal analysis are used to establish solutions of direct and inverse problem between the temperature response vector and heat flux history function of the finite element model. The modal superposition is used to derive the solution of direct problem by combining modal solutions and thermal mode vector of each mode. Then, the inverse problem is derived by using the least square deconvolution with the consideration of dynamic convection effect on estimation result. A novel method of least square deconvolution using recursive concept is introduced to reduce both of the estimation error at discontinuous point of heat flux history and calculation time for least square deconvolution process. Also the experiment result employing commercial heat flux sensor was compared with the estimation result. The accuracy and applicability of estimation method was evaluated by comparing results of experiments in terms of the root mean square error

2. Formulation of the problem

2.1. Thermal modal analysis

An eigenvalue problem in finite element equation of the physical temperature field, $\boldsymbol{T}$ can be expressed by a coupled differential equation with heat capacity matrix $\boldsymbol{C}$ and heat conductance matrix $\boldsymbol{K}$ as Eq. (1)

$$\boldsymbol{K\Phi} = \boldsymbol{C\Phi\Lambda} \tag{1}$$

Here, $\boldsymbol{\Phi}$ is modal matrix and $\boldsymbol{\Lambda}$ is diagonal eigenvalue matrix composed of element $\boldsymbol{\lambda_i}$.

Theoretically, $\boldsymbol{\lambda_i}$ is the reciprocal of the time constant corresponding to the i-th thermal mode, $\boldsymbol{\lambda_i} = \mathbf{1}/\boldsymbol{\tau_i}$, where $\boldsymbol{\tau_i}$ is the time constant of the i-th thermal mode.

The characteristics of the variables in the thermal modal analysis are similar to those in the dynamic modal analysis. One mode includes an eigenvector and eigenvalue of the domain, and each variable is represented by the thermal mode and time constant. Physically, the temperature distribution shapes of thermal modes respond to the thermal load in accordance with the response time determined by their time constants. Also, the entire thermal mode can be used as the basis of the vector space for the temperature solution of direct problem, due to their linear independency. Therefore, the temperature response vector can be introduced by the linear combination of the modal vector and modal solution vector $\boldsymbol{\theta}$.

$$\boldsymbol{T} = \boldsymbol{\Phi\theta} \tag{2}$$

Then, the coupled global finite element equation in the physical temperature field can be written as an equation in the modal temperature field with modal thermal load vector, $\boldsymbol{\zeta_h}$ in which all differential equations are decoupled from each other.

$$\dot{\boldsymbol{\theta}} + \boldsymbol{\Lambda\theta} = \boldsymbol{\Phi}^T\boldsymbol{Q_h} = \boldsymbol{\zeta_h} \tag{3}$$

2.2. Derivation of direct and inverse solution

The concept of a unit load vector for heat input, $\boldsymbol{U_h}$ is applied to the finite element equation to provide information of the location of boundary condition where the surface heat flux is applied. The unit load vector is defined as a thermal load vector which has unity heat flux value at a specific boundary. Therefore, the nodal thermal load vector can be modified into a unit load vector integrated form, $\boldsymbol{\nu} = \boldsymbol{\Phi}^T\boldsymbol{U_h}$, including the unknown heat flux history function, $q(t)$:

$$\dot{\boldsymbol{\theta}} + \boldsymbol{\Lambda\theta} = \boldsymbol{\nu} \cdot q(t) \tag{4}$$

The single set of the first-order differential equation can be expressed as Eq.(5) from the decoupled Eq. (4):

$$\dot{\theta}_i(t) + \lambda_i \cdot \theta_i(t) = \nu_i \cdot q(t) \tag{5}$$

A modal solution corresponding to a specific i-th mode can be solved as Eq. (6) with convolution operator, and the physical solution of the direct problem can be obtained by substituting the modal solution into Eq. (2) as Eq. (7) where the subscript j and m denote the specific node number and total number of modes in the finite element model:

$$\theta_i = \theta_i(0) \cdot e^{-\lambda_i t} + \nu_i \cdot e^{-\lambda_i t} * q(t) \tag{6}$$

$$T_j(t) - T_{j,s}(t) = \left[\sum_{i=1}^{m} \phi_{ji} \cdot \nu_i \cdot e^{-\lambda_i t}\right] * q(t) \tag{7}$$

$$T_{j,s}(t) = \sum_{i=1}^{m} \phi_{ji} \cdot \theta_i(0) \cdot e^{-\lambda_i t} \tag{8}$$

Then the estimation of the surface heat flux history $q(t)$ can be obtained by solving the inverse problem of the direct solution as a deconvolution problem. In the deconvolution of the discrete one dimensional signal, the least square deconvolution method provides a convenient way to obtain the time-dependent solution by considering the convolution as a simple matrix calculation employing the convolution matrix.

To generate the solution of inverse problem, the direct solution is modified into a simple matrix equation by introducing the time series vectors of the temperature responses and the heat flux history function with the convolution matrix $\boldsymbol{H}$:

$$H(t) = \left[\sum_{i=1}^{m} \phi_{ji} \cdot \nu_i \cdot e^{-\lambda_i t}\right] \tag{9}$$

$$T_j(t) - T_{j,s}(t) = H(t) * q(t) \tag{10}$$

$$\boldsymbol{T_j} - \boldsymbol{T_{j,s}} = \boldsymbol{H} \cdot \boldsymbol{q} \tag{11}$$

Then, the least square deconvolution is applied to the direct solution of Eq. (11) to estimate the surface heat flux history vector $\boldsymbol{q}$ by minimizing the least square of the residual vector defined as $\|\boldsymbol{T_j} - \boldsymbol{T_{j,s}} - \boldsymbol{H} \cdot \boldsymbol{q}\|_2^2$ with second-order difference matrix $\boldsymbol{D}$ and the diagonal loading term $k\|\boldsymbol{D} \cdot \boldsymbol{q}\|_2^2$ that aims to avoid the estimation error from the noisy temperature response and problem from the singular of the convolution matrix.

$$\min_{\{q\}} \|\boldsymbol{T_j} - \boldsymbol{T_{j,s}} - \boldsymbol{H} \cdot \boldsymbol{q}\|_2^2 - k\|\boldsymbol{D} \cdot \boldsymbol{q}\|_2^2 \tag{12}$$

$$\boldsymbol{q} = (\boldsymbol{H^T H} + k\boldsymbol{D^T D})^{-1} \cdot \boldsymbol{H^T} \cdot \{\boldsymbol{T_j} - \boldsymbol{T_{j,s}}\} \tag{13}$$

2.3. Consideration of dynamic convection caused by ambient change

In the time-dependent heat flux estimation of the 3D finite domain, the effect of dynamic convection condition should be considered carefully by separating the convectional temperature response from the total response to achieve the accurate result. This is because the estimated heat flux history is highly sensitive to the input vector of the transient temperature response, and every other portions in the input vector except the one from heat flux generate the estimation error directly.

The finite element equation and eigenvalue problem including the boundary conditions of heat flux and convection can be expressed as Eqs. (14) to (15) with their load vectors of $\boldsymbol{Q_h}$ and $\boldsymbol{Q_c}$:

$$\boldsymbol{C\dot{T}} + [\boldsymbol{K_h} + \boldsymbol{K_c}]\boldsymbol{T} = \boldsymbol{Q_h} + \boldsymbol{Q_c} \tag{14}$$

$$[\boldsymbol{K_h} + \boldsymbol{K_c}]\boldsymbol{\Phi} = \boldsymbol{C\Phi\Lambda} \tag{15}$$

Then Eq. (14) also can be introduced into modal equation with the unit load vector of convection boundary condition $\boldsymbol{U_c}$, resulting direct solution of specific node j under the dynamic convection condition in a same way with heat flux boundary condition as shown in Eqs. (16) to (18):

$$\boldsymbol{\zeta_c} = \boldsymbol{\Phi^T U_c} \cdot T_a(t) = \boldsymbol{\varphi} \cdot T_a(t) \tag{16}$$

$$\dot{\boldsymbol{\theta}} + \boldsymbol{\Lambda\theta} = \boldsymbol{\zeta_h} + \boldsymbol{\zeta_c} = \boldsymbol{\nu} \cdot q(t) + \boldsymbol{\varphi} \cdot T_a(t) \tag{17}$$

$$T_j(t) - T_{j,s}(t) = \left[\sum_{i=1}^{m} \phi_{ji} \cdot \nu_i \cdot e^{-\lambda_i t}\right] * q(t) + \left[\sum_{i=1}^{m} \phi_{ji} \cdot \varphi_i \cdot e^{-\lambda_i t}\right] * T_a(t) \tag{18}$$

Substituting $T_{j,c}(t) = \left[\sum_{i=1}^{m} \phi_{ji} \cdot \varphi_i \cdot e^{-\lambda_i t}\right] * T_a(t)$ into Eq. (18), the physical solution of the direct problem under the convection condition can be obtained as:

$$T_j(t) - T_{j,s}(t) - T_{j,c}(t) = H(t) * q(t) \tag{19}$$

$$\boldsymbol{T_j} - \boldsymbol{T_{j,s}} - \boldsymbol{T_{j,c}} = \boldsymbol{H} \cdot \boldsymbol{q} \tag{20}$$

Consequently, the surface heat flux $q(t)$ under dynamic convection with a variable ambient temperature can be estimated by employing the least square deconvolution to Eq. (20):

$$\min_{\{q\}} \|\boldsymbol{T_j} - \boldsymbol{T_{j,s}} - \boldsymbol{T_{j,c}} - \boldsymbol{H} \cdot \boldsymbol{q}\|_2^2 - k\|\boldsymbol{D} \cdot \boldsymbol{q}\|_2^2 \tag{21}$$

$$\boldsymbol{q} = (\boldsymbol{H^T H} + k\boldsymbol{D^T D})^{-1} \cdot \boldsymbol{H^T} \cdot \{\boldsymbol{T_j} - \boldsymbol{T_{j,s}} - \boldsymbol{T_{j,c}}\} \tag{22}$$

2.4. Recursive least square deconvolution for discontinuous input and real-time estimation

The inaccuracy of the heat flux history estimation can be expressed by the approximation limitation of the source form of the estimation equation. As described in Eq. (18) and Eq. (22), the inverse solution is obtained by employing the direct physical solution of the nodal temperature composed of the combinations of exponential functions with different time constants. Hence, the estimation result of discontinuous heat flux history cannot be properly produced based on the assumption of the inverse solution form combining a finite number of different exponential functions.

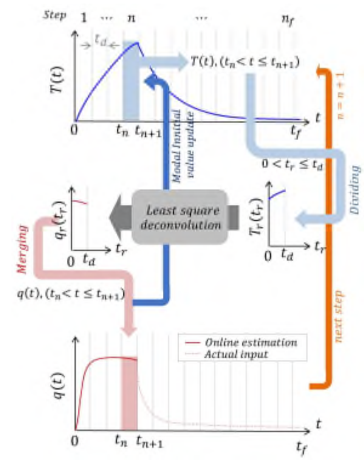

Figure 1. Schematics of recursive least square deconvolution procedure

The computational load of the inverse solution for long-term estimation is another limitation of least square deconvolution. The size of the convolution matrix $\boldsymbol{H}$ is determined by the estimation time range and time step, therefore, the long-term estimation requires a large convolution matrix and also the large computational load.

The recursive approach for the inverse solution is introduced to achieve an accurate estimation around discontinuous points in the actual heat flux history function and efficient computing for the real-time heat flux history estimation.

Fig. 1 depicts the procedure of recursive least square deconvolution. The temperature measurement and estimation result are divided by several recursive steps with a specified recursive time duration t_d and recursive time step dt_r to reduce the time range for each recursive step. Then, Eq. (24) can be changed into the recursive direct solution and recursive least square deconvolution as in the same way with the total inverse solution. Consequently, the size of convolution matrix for each recursive step $\boldsymbol{H_r}$ can be drastically reduced according to the recursive time duration and recursive time step.

The modal initial value for next recursive step $\theta_i(t_d)$ is updated using the analytic modal solution with the estimated heat flux history function of the present step and triggers the next recursive step. With this recursive concept, estimation result in each recursive step can be considered as independent function, so the estimation result more accurately follows the discontinuous points. Moreover, the real-time calculation with specified recursive time duration can be employed by the recursive estimation algorithm due to the reduced size of the convolution matrix for each recursive step.

3. Experiment

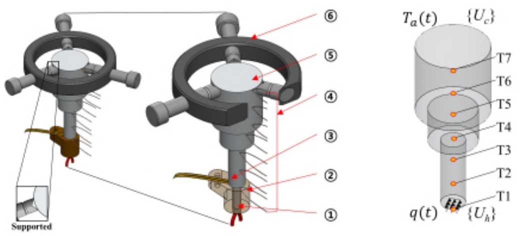

Figure 2. Schematics of the experiment setup: 1. heater, 2. heater jig, 3. heat flux sensor, 4. thermocouples, 5. specimen, 6. mount jig

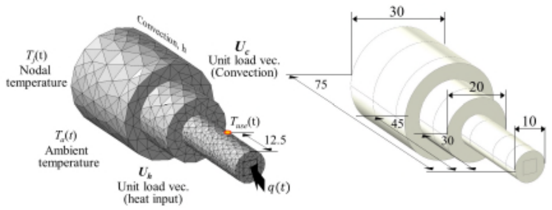

Figure 3. Schematics of specimen for FE model and experiment

The experiment setup is depicted in Fig. 2. The experiments were performed using a ceramic heater to liberate the heat to the aluminium specimen mounted on a three-point jig. The commercial thermopile-type heat flux sensor was placed between the ceramic heater and specimen to measure the applied surface heat flux, and K-type thermocouples were attached to surface of the specimen with 14 mm of uniform space to measure the transient temperature response of the specimen. The test setup was placed in a transparent chamber to prevent any external disturbance around the specimen, and a plastic thermal insulator was installed between the mounting jig and specimen to reduce the heat flow from the specimen to mounting jig. The change in ambient temperature of the chamber was monitored by the thermocouples, allowing application of a variable ambient temperature. Fig. 4(a) presents the transient temperature response of the specimen from seven thermocouples during the heating and cooling state. The maximum temperature change from the initial temperature 25 ºC reaches 45 ºC at the T1 position. Fig. 4(b) shows the average change in the ambient temperature measured by four thermocouples in the chamber. Also, the ambient temperature condition was intentionally decreased from 25 ºC to 21 ºC to compare the effect of dynamic convection condition on estimation result as described in Eqs. (18)-(22) and measured temperature change data was applied to heat flux estimation model as ambient temperature history $T_a(t)$.

Table 1 Estimation result comparison of figure 4.

Figure	(a)	(b)	(c)	(d)
RMSE $[kW/m^2]$	1.37	5.50	24.28	0.12
Ratio [%]	2.3	9.3	41.0	0.2

Table 2 Computational time of the each method

Estimation Method	LSD Entire time $dt = 0.1s$	RLSD $t_d = 25s$ $dt_r = 0.01$s	RLSD $t_d = 25s$ $dt_r = 0.1s$
Time	3h 20m	10m 23s	49s

The commercial finite element analysis software COMSOL was used to generate the $\boldsymbol{C}$ and $\boldsymbol{K}$ with other unit load vectors.

Figs. 5(a) and 5(b) compare the estimation accuracy in the presence of the convection effect. The estimation result with a dynamic convection condition, Fig. 5(a), shows 1.37 kW/m^2 RMSE representing 2.3% of the maximum measured value and a reasonable difference between the estimated and measured one. In contrast, Fig. 5(b) depicts an inaccurate estimation result, including 5.5 kW/m^2 RMSE value with gradually increasing error. The estimation error in Fig. 5(b) shows a similar transient trend with the excluded ambient temperature measurement result, which indicates that the estimation error in the 3D finite domain can be fairly produced by the absence of the dynamic convection condition in the estimation equation.

The estimation result employing the conventional transient surface heat flux history estimation method based on the Stoltz algorithm is compared with the measured result in Fig. 5(c). The estimation error is considerably larger than the suggested method, with 24.28 kW/m^2 RMSE. This result shows the typical estimation error for the conventional method based on the simplified dimension of the target geometry. Maximum amplitudes in the heat flux during the heating state of both the RLSD and Stoltz results are 59.2 kW/m^2 and 15.8 kW/m^2, respectively, and this amplitude difference originated from the area difference of the heat flux boundary between the actual experimental setup and the Stoltz method. The actual area of the surface heat flux boundary is 19.3 mm^2, as shown by the rectangular range in Fig. 3, but the Stoltz method does not account for the separated surface heat flux zone, so the algorithm estimates the result by considering the boundary area to be the entire surface at the end of the specimen. Also, the estimate result from the Stoltz method shows negative error at a cooling range, caused by the absence of the convection condition.

Table 2 compares the computational times for each least square deconvolution condition and all computation was realized in a PC with 3GHz Intel i5 CPU(8500) and 4Gb memory. It can be observed that, for the entire time, the least square deconvolution requires over 3 hours to produce the estimation result. This is because the long-term least square deconvolution requires a large convolution matrix that consumes computational resources. On the other hand, the recursive least square deconvolution takes only 49 seconds for same time step as recursive time step of 0.1 seconds and 11 minutes for 0.01 seconds of recursive time step.

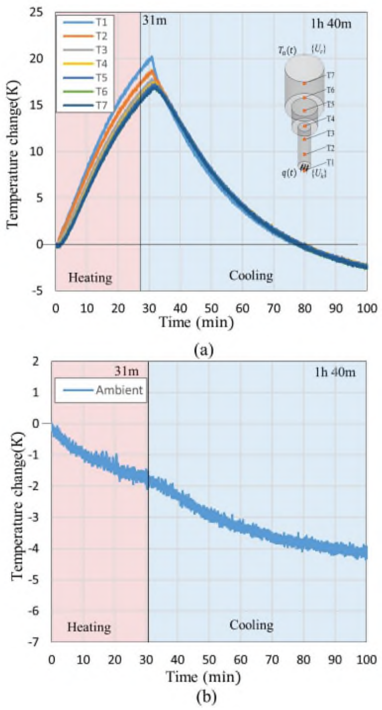

Figure 4. Temperature measurement result:
(a) Temperature response of specimen
(b) Temperature change in chamber

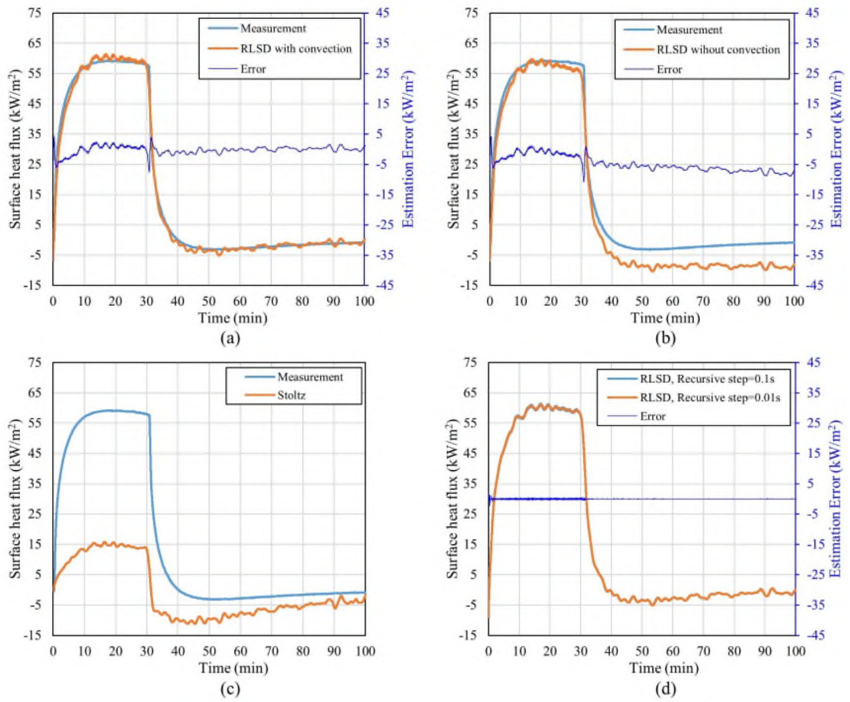

Figure 5. Estimation result comparison of the surface heat flux with the measurement result: (a) With measurement, (b) variable ambient temperature effect on estimation (c) estimation result comparison with the Stoltz method, (d) estimation result with different recursive time step

4. Conclusion

In the present study, the solution for the inverse heat conduction problem is derived by employing both the thermal modes from a finite element model and the recursive least square deconvolution, so that the real-time estimation and accurate estimation around the discontinuous heat flux history can be achieved for 3D finite domain.

The solution to the direct problem is derived by the modal superposition of the thermal modes and modal solution containing the reciprocal of the time constant in each mode. Then, the solution to the inverse problem can be obtained by applying the least square deconvolution to the direct solution.

The proposed estimation method was evaluated for two points by comparing the measured surface heat flux history from experiment with the estimated one. First, the consideration of the dynamic convection improves the estimation accuracy for the 3D finite domain. The RMSE between the measured and estimated surface heat flux history shows $1.37\ kW/m^2$, indicating only 2.3% level for maximum measured surface heat flux history. Second, the computing time for estimation is significantly reduced from 3 hour 20 minutes to only 49 seconds by employing proposed RLSD method which allows real-time surface heat flux history estimation.

Acknowledgment

The research was supported by the Development of Core Technologies for Transportation Systems-Green Car program (10070201) funded by the MOTIE of Korea.

References

[1] Kim Y Y, Kim G H, and Lee S K 2019 Real-time estimation of time-dependent heat flux for 3D finite domain employing thermal mode and recursive least square deconvolution Int. *J. Heat Mass Transf.* **144** 118622-31

[2] Hutton D V 2004 Fundamental of Finite Element Analysis Tata McGraw-Hill New York

[3] Zhu J, Ni J, Shih A J, 2008 Robust Machine Tool Thermal Error Modeling Through Thermal Mode Concept *J. Manuf. Sci. Eng.* **130**(6) 061006-9

[4] Lawson C L and Hanson R J 1987 Solving Least Squares Problems SIAM

[4] Logan D L 2002 A first course in the finite element method Brooks/Cole USA

[4] Beck Inverse J V 1985 heat conduction ill-posed problem Wiley USA